A LOW-FREQUENCY SUPERDIRECTIVE ACOUSTIC VECTOR SENSOR ARRAY

*Xijing Guo**

Northwestern Polytechnical University
School of Marine Science and Technology
127 Youyi Xilu, 710072 Xi'an, China
xijing.guo@gmail.com

Shie Yang, Hu Zhang

Harbin Engineering University
Acoustic Science and Technology Laboratory
145 Nantong Street, 150001 Harbin, China
zhanghu@hrbeu.edu.cn

ABSTRACT

This paper provides a novel acoustic vector sensor array architecture for superdirectivity at low frequencies. It has a uniform 3 by 3 rectangular geometry of intersensor spacing less than 0.04 wavelength over its operation frequency band, with an up to 10.4 dB of directivity index in cylindrically isotropic noise. This is realized through a mode domain approach, which accesses the acoustic modes by fitting certain multipole models to the wavefield observations. Field experiments show that this is a practical solution of implementing a miniaturized vector sensor array with superdirectivity.

Index Terms— Acoustic vector sensor, multipole, beamforming, superdirectivity, array signal processing.

1. INTRODUCTION

For passive underwater acoustic surveillance, the operation frequency band generally ranges from a few tens to a few hundreds of Hertz. Under these circumstances, setting the intersensor spacing at one-half wavelength leads to a huge array aperture, making deployment and maintenance of such a sensor array prohibitively difficult.

Meyer and Elko [1] introduced the mode domain beamforming, or simply "modal beamforming", for a miniaturized differential spherical sensor array to achieve higher order directivity. The acoustic "mode" is referred as the standing wave components in the wavefield. This concept attracts much attention and hitherto there have been many superdirective differential array designs [2]-[5]. However, these approaches do not apply straightforwardly in the case of acoustic vector sensors (AVS), which have the first order directivity by nature. For the last two decades the AVS arrays have been extensively studied and tested [6]-[13]. Nevertheless, the overwhelmingly majority of these designs are still restricted to the half wavelength intersensor spacing constraint.

The first differential AVS array without the half wavelength spacing constraint was probably due to Franklin [14]. As a linear array, it suffers from the inconvenience that the main response axis can not be steered, which has been solved very recently by Gur [15]. For the two-dimensional (2-D) acoustic field, Zou and Nehorai [16] developed a mode domain approach to gain superdirectivity on a circular differential vector sensor array. The 2-D symmetric architecture ensures its main response axis to be steered freely.

This paper provides a uniform rectangular vector sensor array with superdirectivity subject to a miniaturized aperture. We base our method on fitting the multipole models to the differentially processed acoustic particle velocity component measurements, for the reason that a multipole is directional but infinitely small in physical dimension. The multipole models have also been used for superdirective beamforming by McConnell *et al.* [17] and by Eichler and Lacroix [18]. However, in these pioneer works the sensors are the omnidirectional pressure sensors and the array geometry is limited to a circular shape.

2. RECTANGULAR ARRAY ARCHITECTURE

Consider the horizontal 3×3 uniform rectangular sensor array of intersensor spacing a shown in Fig. 1. The sensor at the center of the array is chosen as the reference. All these sensors are biaxial vector sensors, providing measurements of the particle velocity components of the acoustic wave field along both the x and the y directions. Slightly different from the others, in the package of the reference sensor it also comprises a pressure sensor.

Similar to [16], it is a 2-D acoustic field in the shallow water environment, where the vector sensor array is restricted to scan the horizontal surface. Assume that a narrowband acoustic plane wave arrives from the angle ϕ at speed c. The frequency ω is very low such that $ka \ll 1$ where $k = \omega c^{-1}$ is the wave number. In contrast, the half wavelength intersensor spacing requirement implies $ka = \pi$. The array manifold can

*This work is supported by the State Key Laboratory of Acoustics, Institute of Acoustics, Chinese Academy of Sciences, the National Natural Science Foundation of China under Grant 11304251, the Specialized Research Fund for the Doctoral Program of Higher Education of China under Grant 20136102120014, and the Northwestern Polytechnical University Foundation for Fundamental Research under Grant JCY20130106.

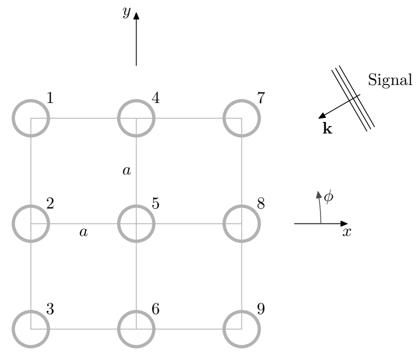

Fig. 1. Top view of the geometry of the vector sensor array. A circle represents a vector sensor, indexed from 1 to 9.

be written as a 9×1 vector $\mathbf{a}(\phi) = \mathbf{a}_x(\phi) \otimes \mathbf{a}_y(\phi)$, where

$$\mathbf{a}_y(\phi) = \begin{bmatrix} e^{-ika\sin\phi} \\ 1 \\ e^{+ika\sin\phi} \end{bmatrix} \quad \mathbf{a}_x(\phi) = \begin{bmatrix} e^{+ika\cos\phi} \\ 1 \\ e^{-ika\cos\phi} \end{bmatrix}$$

and $\otimes$ denotes the Kronecker (element-wise) product. We denote the incident wave by $s(t)$. At the receiver, the observations include the sound pressure component $p(t)$, the particle velocity components along the x-axis, denoted by the 9×1 vector $\mathbf{v}_x(t) = [v_{x,1}(t), \ldots, v_{x,9}(t)]^T$ and the other 9 components along the y-axis, $\mathbf{v}_y(t) = [v_{y,1}(t), \ldots, v_{y,9}(t)]^T$. A compact formulation of these observations reads

$$\mathbf{z}(t) = \begin{bmatrix} p(t) \\ \mathbf{v}_x(t) \\ \mathbf{v}_y(t) \end{bmatrix} = \begin{bmatrix} 1 \\ \begin{bmatrix} \cos\phi \\ \sin\phi \end{bmatrix} \otimes \mathbf{a}(\phi) \end{bmatrix} s(t) + \mathbf{n}(t)$$

where $\mathbf{n}(t)$ denotes the noise. For notational simplicity, the dependence of a signal on t will be often omitted in the sequel.

3. SUPERDIRECTIVE BEAMFORMING

The notion "modal beamforming" coined by Meyer and Elko [1] was extended recently to the vector sensor case by Zou and Nehorai [16] where the 2-D acoustic field was considered. In that 2-D case, the spherical array of omnidirectional sensors [1] was substituted by the vector sensors configured on a circular grid. Similar to the circular array case, for the uniform rectangular vector sensor array herein, superdirectivity is also achieved through two steps, *i.e.*, the mode extraction and synthesis. However, it needs an extra "decoupling" step to cancel the errors due to the finite difference, which is the base of the mode extraction step herein. The three steps will be described as follows.

3.1. Mode Extraction

Observe that the pressure measurement at the reference sensor provides a natural estimate of the 0th mode of the acoustic field. Hence, we only need to derive the modes of orders $1 \leq n \leq N$ from the observations of the particle velocity components along both the x and the y axes received at the L positions. We define a $2N \times 2L$ block diagonal matrix of weights

$$\mathbf{G} = \mathbf{I}_2 \otimes (\mathbf{\Gamma}\bar{\mathbf{G}})$$

where $\mathbf{I}_2$ denotes the 2nd order identity matrix. It links the $2L$ particle velocity components, denoted by $\mathbf{v} = [\mathbf{v}_x^T, \mathbf{v}_y^T]^T$, to a $2N \times 1$ vector $\mathbf{u} = [\bar{u}_1, \ldots, \bar{u}_N, \tilde{u}_1, \ldots, \tilde{u}_N]^T$ as

$$\mathbf{u} = \mathbf{G}\mathbf{v}. \tag{1}$$

For the 3×3 uniform vector sensor array, it is obvious that $L = 9$ and in this paper the highest order of the modes is given by $N \leq 5$. Let $\kappa = ika$. The choice of $\mathbf{\Gamma} = \operatorname{diag}\left(1, \kappa^{-1}, \kappa^{-2}, 4\kappa^{-3}, 16\kappa^{-4}\right)$ is a 5×5 diagonal matrix

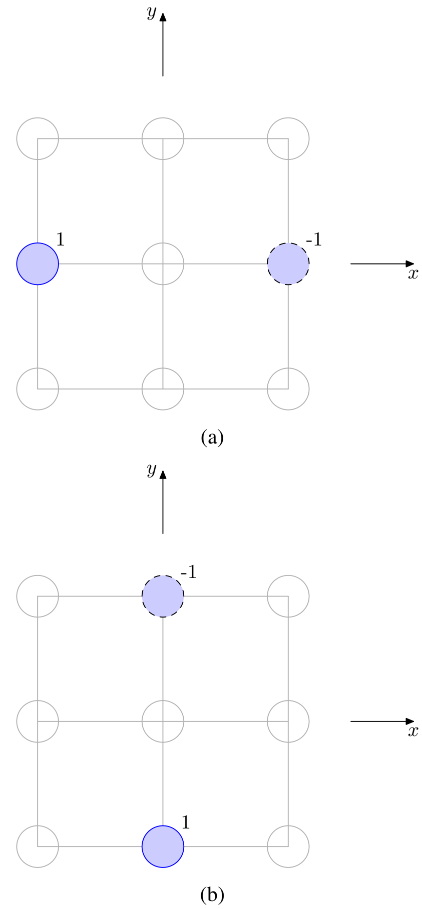

Fig. 2. Illustration of the weights associated to the sensor positions for the 2nd order mode. The highlighted circles in color denote the enabled sensor, otherwise are those weighed by 0. The digit to the upper right of the sensor is the weight associated to it, where the sensor with positive weight is marked by the solid circle and negative weight by the dashed circle.

Table 1. Results of the Transform (1)

Order n	1	2	3	4	5
$\bar{u}_n$	$\cos\phi$	$1+\cos 2\phi$	$\cos\phi+\cos 3\phi$	$-1+\cos 4\phi$	$-2\cos\phi+\cos 3\phi+\cos 5\phi$
$\tilde{u}_n$	$\sin\phi$	$\sin 2\phi$	$-\sin\phi+\sin 3\phi$	$-2\sin 2\phi+\sin 4\phi$	$-2\sin\phi-\sin 3\phi+\sin 5\phi$

of typical element γ_n and $\bar{\mathbf{G}}$ is given by the 5×9 matrix

$$\bar{\mathbf{G}} = \begin{bmatrix} 0 & 0 & 0 & 0 & 1 & 0 & 0 & 0 & 0 \\ 0 & 1 & 0 & 0 & 0 & 0 & 0 & -1 & 0 \\ 0 & 2 & 0 & -2 & 0 & -2 & 0 & 2 & 0 \\ -1 & 2 & -1 & 0 & 0 & 0 & 1 & -2 & 1 \\ -1 & 2 & -1 & 2 & -4 & 2 & -1 & 2 & -1 \end{bmatrix}.$$

The nth row of $\bar{\mathbf{G}}$ is deduced from the perspective of fitting the nth order multipole model, associated with the nth mode, to the particle velocity observations from the 9 sensor positions. For example, we illustrate the 2nd row of $\bar{\mathbf{G}}$ by highlighting the sensor positions associated to nonzero weights in Fig. 2(a), which clearly shows a realization of the dipole model. The finite difference of the particle velocity components along the x-axis from the two enabled sensors equals

$$\begin{aligned} \bar{u}_2 &= \gamma_2(-e^{-ika\cos\phi}\cos\phi + e^{ika\cos\phi}\cos\phi) \\ &= 2i\kappa^{-1}\cos\phi\sin(ka\cos\phi) \qquad (2) \\ &\approx 2\cos^2\phi \end{aligned}$$

where the approximation derives from the fact that

$$\sin(ka\cos\phi) \approx ka\cos\phi$$

for $ka < 0.25$. Equation (2) can be further expressed as $\bar{u}_2 \approx 1 + \cos 2\phi$. Attention should be paid to the $\cos 2\phi$ term, which is exactly the cosine component of the 2nd order mode. Obviously, such a transform is nonlinear, whereas the wavefield decomposition used in the circular array case [16] is a linear transform. We can also deduce $\tilde{u}_2 \approx \sin 2\phi$ by a similar argument, which provides the sine component of the 2nd order mode. For the higher order modes, it is similar, which follows the radiation of the lateral quadrupole, the octupole, and so forth. Therefore, the relation (1) can be understood as a transform that maps the observations of the acoustic field to the mode domain. The results are tabulated in Table 1.

It should be pointed out that the matrix $\mathbf{G}$ is not the only solution to the mode domain transform. For example, Fig. 2(b) illustrates an alternative realization of a dipole, from which we can also derive another set of weights for the 2nd order mode. More solutions can be obtained in a similar manner.

3.2. Decoupling

From Table 1 we observe that for the rectangular array the modes extracted from the observations are not necessarily "pure". This is understood as coupling between the modes due to the finite difference errors. To eliminate these errors, the pressure observation, *i.e.*, the 0th order mode, is used to decouple the higher order modes. The decoupling can be formulated by a block diagonal matrix

$$\mathbf{D} = \begin{bmatrix} \mathbf{D}_1 & \\ & \mathbf{D}_2 \end{bmatrix}_{11\times 11}$$

where the two blocks $\mathbf{D}_1$ and $\mathbf{D}_2$ are respectively given by a 6×6 and a 5×5 lower triangular matrices

$$\mathbf{D}_1 = \begin{bmatrix} 1 & & & & & \\ 0 & 1 & & & & \\ -1 & 0 & 1 & & & \\ 0 & -1 & 0 & 1 & & \\ 1 & 0 & 0 & 0 & 1 & \\ 0 & 3 & 0 & -1 & 0 & 1 \end{bmatrix}$$

and

$$\mathbf{D}_2 = \begin{bmatrix} 1 & & & & \\ 0 & 1 & & & \\ 1 & 0 & 1 & & \\ 0 & 2 & 0 & 1 & \\ 3 & 0 & 1 & 0 & 1 \end{bmatrix}.$$

The decoupling step renders a $(2N+1) \times 1$ vector

$$\begin{aligned} \mathbf{h}(\phi) &= \begin{bmatrix} 1 & \\ & 2\mathbf{I}_{2N} \end{bmatrix} \mathbf{D} \begin{bmatrix} 1 & \\ & \mathbf{G} \end{bmatrix} \mathbf{z} \\ &= [1, 2\bar{h}_1(\phi), \ldots, 2\bar{h}_N(\phi), 2\tilde{h}_1(\phi), \ldots, 2\tilde{h}_N(\phi)]^T, \end{aligned}$$

where $\bar{h}_n(\phi) \approx \cos(n\phi)$ and $\tilde{h}_n(\phi) \approx \sin(n\phi)$, providing the estimates of the $2N+1$ mode components.

3.3. Synthesis

The synthesis step is exactly the same as that of the circular array case. The vector of the $2N+1$ mode components $\mathbf{h}(\phi)$ is projected to the $(2N+1) \times 1$ steering vector

$$\mathbf{w}(\alpha) = [1, \cos(\alpha), \ldots, \cos(N\alpha), \sin(\alpha), \ldots, \sin(N\alpha)]^T$$

where α is the steering angle, yielding

$$G(\phi) = \mathbf{w}^T(\alpha)\mathbf{h}(\phi) \approx \frac{\sin\frac{2N+1}{2}(\phi-\alpha)}{\sin\frac{1}{2}(\phi-\alpha)}.$$

Such a beam pattern has been shown to have the the maximum directivity in the 2-D isotropic noise [19].

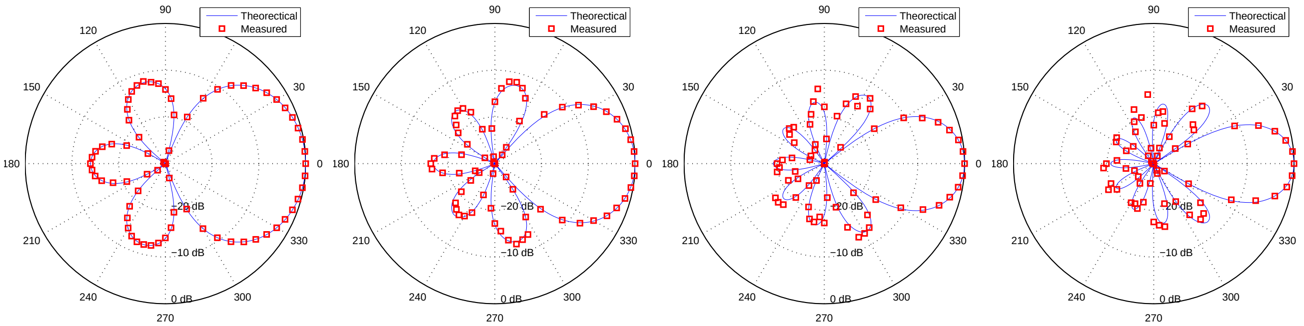

(a) $N = 2$ (b) $N = 3$ (c) $N = 4$ (d) $N = 5$

Fig. 3. Measured beam patterns at 170 Hz in the anechoic water tank for $2 \leq N \leq 5$.

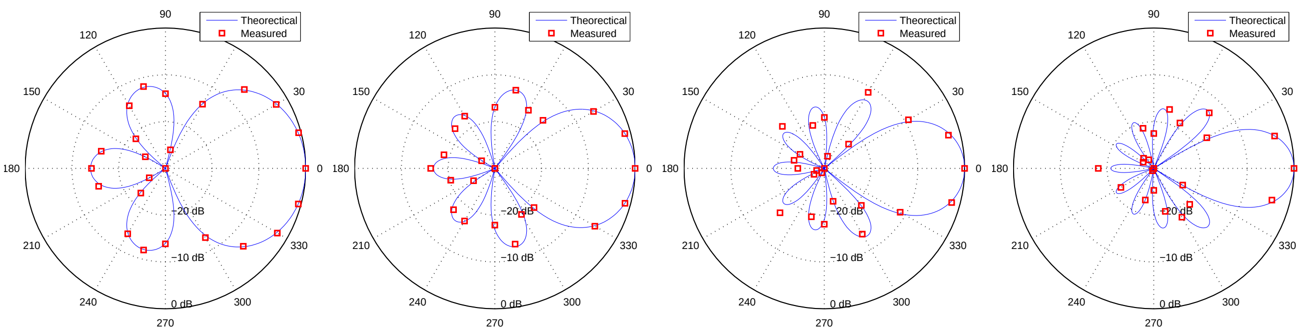

(a) $N = 2$ (b) $N = 3$ (c) $N = 4$ (d) $N = 5$

Fig. 4. Measured beam patterns at 170 Hz in the lake for $2 \leq N \leq 5$.

For $N = 5$, it is immediate from the beam pattern expression that the 3 dB beamwitdth is approximately $29.09°$ and the first sidelobe is -13.02 dB, occurring at $\phi = \alpha \pm 46.94°$. Furthermore, the 2-D directivity index (DI) is given by

$$DI = 10 \log_{10} \frac{2\pi}{\displaystyle\int_0^{2\pi} \left[\frac{G(\phi)}{2N+1} \right]^2 d\phi} \approx 10 \log_{10}(2N+1),$$

which is approximately 10.4 dB.

4. EXPERIMENTS

A prototype of the 3×3 vector sensor array has been developed for the experiments. The intersensor spacing is fixed to $a = 0.12$ m such that the array aperture is constrained to less than 0.5 m. The array was tested first in a water tank, which is not really anechoic within the interested frequency band. A sound source was fixed in the far field of the array, transmitting rectangular continuous wave pulses. The pulses were repeated at every second and each pulse lasted 20 cycles in terms of the frequency of the continuous wave, or the carrier. At the receiver, the vector sensor array was rotated around the z-axis with an angular step of $5°$. A time window is used to truncate the received signals to suppress the interference caused by the reverberant environment in the time domain. Then, the measured steering vectors were used to form the desired beam patterns. The beamforming results at 170 Hz, averaged over 15 pulses, are shown in Fig. 3, where the main response axis is steered at the direction of $0°$. It can be observed that the measured beam patterns, denoted by the discrete squares, well agree with the theoretical beam patterns.

We also carried out several experiments in a lake of southern China, 2013, which provides a less reverberant environment compared to the water tank. The experiment setup was largely reproduced in the lake except that during these experiments the array was rotated with a $15°$ angular step to save time. For comparison purposes, the results at 170 Hz are also presented, as shown in Fig. 4. It clearly shows that a practical superdirective beam pattern is obtained.

5. CONCLUSION

A miniaturized 3×3 uniform rectangular vector sensor array with superdirectivity has been developed. The method is based on realizations of the multipole models up to the 5th order with certain combinations of the vector sensors. Experiments show that it is practical to achieve a directivity index of 10.4 dB with this 3×3 vector sensor array in the 2-D acoustic field.

6. REFERENCES

[1] J. Meyer and G. Elko, “A highly scalable spherical microphone array based on an orthonormal decomposition of the soundfield,” in *Proc. IEEE ICASSP*, vol. 2, Orlando, FL, USA, May 2002, pp. 1781–1784.

[2] B. Rafaely, “Anaysis and design of spherical microphone arrays,” *IEEE Trans. Speech Audio Process.*, vol. 13, no. 1, pp. 135–143, Jan. 2005.

[3] H. Teutsch and W. Kellermann, “Acoustic source detection and localization based on wavefield decomposition using circular microphone arrays,” *J. Acoust. Soc. Am.*, vol. 120, no. 5, pp. 2724–2736, Nov. 2006.

[4] Z. Li and R. Duraiswami, “Flexible and optimal design of spherical microphone arrays for beamforming,” *IEEE Trans. Speech Audio Process.*, vol. 15, no. 2, pp. 702–714, Feb. 2007.

[5] E. De Sena, H. Hacihabiboglu, and Z. Cvetkovic, “On the design and implementation of higher order differential microphones,” *IEEE Trans. Speech Audio Process.*, vol. 20, no. 1, pp. 162–174, Jan. 2012.

[6] A. Nehorai and E. Paldi, “Acoustic vector-sensor array processing,” *IEEE Trans. Signal Process.*, vol. 42, no. 9, pp. 2481–2491, Sep. 1994.

[7] K. T. Wong and M. D. Zoltowski, “Self-initiating MUSIC-based direction finding in underwater acoustic particle velocity-field beamspace,” *IEEE J. Oceanic Eng.*, vol. 25, no. 2, pp. 262–273, Mar. 2000.

[8] J. C. Shipps and B. M. Abraham, “The use of vector sensors for underwater port and waterway security,” in *Proc. Sensors Industry Conf.*, New Orleans, LA, Jan. 2004, pp. 41–44.

[9] J. C. Nickles, G. Edmonds, R. Harriss, F. Fisher, W. S. Hodgkiss, J. Giles, and G. D’Spain, “A vertical array of directional acoustic sensors,” in *Proc. OCEANS*, vol. 1, Newport, RI, Oct. 1992, pp. 340–345.

[10] G. L. D’Spain, W. S. Hodgkiss, G. L. Edmonds, J. C. Nickles, F. H. Fisher, and R. A. Harriss, “Initial analysis of the data from the vertical DIFAR array,” in *Proc. OCEANS*, vol. 1, Newport, RI, Oct. 1992, pp. 346–351.

[11] V. A. Shchurov and M. V. Kuyanova, “Use of acoustic intensity measurements in underwater acoustics (modern state and prospects),” *Chin. J. Acoust.*, vol. 18, no. 4, pp. 315–326, 1999.

[12] J. F. McEachern, J. A. McConnell, J. Jamieson, and D. Trivett, “ARAP - deep ocean vector sensor research array,” in *Proc. OCEANS*, Boston, MA, Sep. 2006.

[13] G. L. D’Spain, J. C. Luby, G. R. Wilson, and R. A. Gramann, “Vector sensors and vector sensor line arrays: Comments on optimal array gain and detection,” *J. Acoust. Soc. Am.*, vol. 120, no. 1, pp. 171–185, Jul. 2006.

[14] J. B. Franklin, “Superdirective receiving arrays for underwater acoustic application,” Defence Research Establishment Atlantic, Dartmouth, Canada, DREA Contractor Report 97/444, 1997.

[15] B. Gur, “Particle velocity gradient based aoustic mode beamforming for short linear vector sensor arrays,” *J. Acoust. Soc. Am.*, vol. 135, no. 6, pp. 3463–3473, Jun. 2014.

[16] N. Zou and A. Nehorai, “Circular acoustic vector-sensor array for mode beamforming,” *IEEE Trans. Signal Process.*, vol. 57, no. 8, pp. 3041–3052, Aug. 2009.

[17] J. A. McConnell, S. C. Jensen, and J. P. Rudzinsky, “Forming first- and second-order cardioids with multimode hydrophones,” in *Proc. OCEANS*, Boston, MA, Sep. 2006.

[18] M. Eichler and A. Lacroix, “Broadband superdirective beamforming using multipole superposition,” in *Proc. EUSIPCO*, Lausanne, Switzerland, Aug. 2008.

[19] B. A. Cray and A. H. Nuttall, “Directivity factors for linear arrays of velocity sensors,” *J. Acoust. Soc. Am.*, vol. 110, no. 1, pp. 324–331, Jul. 2001.